A Time Diversity Model for EHF Satellite Communication Systems

Lorenzo Luini, *Senior Member*, *IEEE*, Alberto Panzeri,
Carlo Riva, *Senior Member*, *IEEE*, Domingo Pimienta-del-Valle, José Manuel Riera, *Senior Member*, *IEEE*

***Abstract* – A simple yet effective time diversity model, referred to as TD-SCEX, is presented. The model, conceived to support the design of EHF Earth–space communication systems implementing Fade Mitigation Techniques, takes advantage of the SC EXCELL model to predict the joint rain attenuation statistics, hence the time diversity gain, starting from the geometrical and electrical characteristics of the link, as well as from the joint rain rate statistics. The model performance is evaluated against the data collected in Milan, Madrid and Spino d'Adda at Ka, Q and V bands, in the framework of different long-term propagation campaigns. Results indicate that TD-SCEX is a useful tool to predict the effectiveness of time diversity in improving the performance of EHF Earth-space communication systems.**

***Index Terms* — Tropospheric attenuation, rain attenuation, fade mitigation techniques, time diversity, satellite communications, prediction model.**

I. Introduction

Among the tropospheric effects impairing the propagation of electromagnetic waves in the troposphere, the attenuation due to rain prevails at any frequency above approximately 10 GHz [1]. Satellite and terrestrial telecommunication operators are more and more interested in high frequency bands (i.e. Ka and above, up to the W band) because of the advantage of using larger bandwidths and smaller equipment, but at the same time, they need to cope with stronger fades, which cannot always be counteracted by resorting to the fixed margins. The alternative approach to guarantee high system availability and the target Quality of Service is to use suitable Fade Mitigation Techniques [2], like time diversity, which is the focus of this work [3]. This technique consists in repeating the transmission of the same information with a predetermined time lag Δt, after which the receiver can select, ideally on an instantaneous basis, the best samples contained in the 'main' time series or in the delayed copy of it, i.e. the ones subject to less rain attenuation. For instance, time diversity would not be suitable for real-time applications, but it would be definitely useful for systems aimed at asynchronous data transfer (e.g. file download).

For design purposes, the advantage originating from the implementation of time diversity can be evaluated using rain attenuation time series collected in the framework of radio wave propagation experiments [4]. In sites where measurements are not available, and in any case, at frequencies beyond 49.5 GHz (the maximum one ever used in satellite propagation experiments [5]), prediction methodologies can be used. A typical modeling approach is to take advantage of rain rate measurements collected using local sensors to be used as input to physically based methods, such as the Synthetic Storm Technique [6], for the simulation of time series of rain attenuation affecting Earth-space links with different characteristics. Using a similar approach, rain maps, either synthesized by a model like MultiEXCELL [7] or derived from weather radars with a suitable temporal resolution, can be employed to obtain time series of rain attenuation across mid-scale areas [8]. Though effective, simulations methodologies are complex, time consuming, and relying on input data that might not be easily available in several sites (e.g. radar ones). Alternatively, analytical models can be used, such as the statistical one presented in [9], which relies on the assumption that rain attenuation is a lognormal random variable.

This analytical model was compared in [4] with some other models (namely: the ones proposed by Matricciani [6], Greece [10] and ONERA [11]) to assess their performance using as reference Ka- and Q-band experimental data gathered at Madrid for a three-year period. The model proposed in [9] was indeed found to give the best results, but only after regressing the needed parameters on the experimental data. Moreover, recently, an empirical model was presented in [12] based on Ka- and Q-band data from a two-year experiment at Aveiro, Portugal, using a second order polynomial fitting.

This contribution presents a simple yet effective analytical model, hereinafter referred to as TD-SCEX (Time Diversity Stratiform Convective EXCELL), aimed at estimating the advantage of implementing time diversity in EHF Earth-space

Manuscript received XXXX. This work was supported in part by the Ministry of Science, Innovation and Universities of Spain through the RTI2018-098189-B-I00 project.

Lorenzo Luini and Carlo Riva are with the Dipartimento di Elettronica, Informazione e Bioingegneria, Politecnico di Milano, Piazza Leonardo da Vinci, 32, 20133, Milano, Italy, and with the Istituto di Elettronica e di Ingegneria dell'Informazione e delle Telecomunicazioni (IEIIT), Consiglio Nazionale delle Ricerche, Via Ponzio 34/5, Milano 20133, Italy (e-mail: lorenzo.luini@polimi.it).

Alberto Panzeri is with the Dipartimento di Elettronica, Informazione e Bioingegneria, Politecnico di Milano, Piazza Leonardo da Vinci, 32, 20133, Milano, Italy.

José Manuel Riera and Domingo Pimienta-del-Valle are with Information Processing and Telecommunications Center, Universidad Politécnica de Madrid, ESTI de Telecomunicación, Av. Complutense, 30, 28040, Madrid, Spain.

communication systems. The model consists of two steps: the calculation of joint rain rate statistics, for given time lags, starting from the rain rate time series; the use of such statistics as input to the SC EXCELL (Stratiform Convective EXponential CELL) model, which, presented in [13], aims at estimating rain attenuation statistics for Earth-space links starting from a site-tailored population of synthetic rain cells [14] and considering the different impact of stratiform and convective precipitation on the link. The accuracy of the results obtained by applying such a methodology is evaluated against the propagation data collected in three sites (Milan, Madrid and Spino d'Adda) using beacon signals broadcast by three satellites (Alphasat, KA-SAT and ITALSAT) at three different bands (Ka, Q and V).

The remainder of this paper is structured as follows. Section II presents the experimental equipment, Section III describes how the experimental rain rate and rain attenuation time series are processed; TD-SCEX is outlined in Section IV, while Section V presents the results and evaluates the accuracy of TD-SCEX, which is also compared to the one achieved by other models in the literature. Finally, Section VI draws some conclusions.

II. Experimental Equipment

This section presents the experimental equipment used to collect the data, drawn from satellite-based radio wave propagation experiments conducted in three sites, used in this work to assess the accuracy of TD-SCEX.

A. Milan

The Milan data were collected during 2017 and 2018 in the framework of the Alphasat Aldo Paraboni propagation experiment [15]. The space segment of the experiment includes the Alphasat satellite, a geosynchronous satellite owned by Inmarsat (25° East orbital position), which carries the Aldo Paraboni payload, featuring two continuous-wave beacons at 19.7 GHz and 39.4 GHz. Since 2014, Politecnico di Milano collaborates with NASA (Glenn Research Centre), which has installed in the main university campus (latitude 45.48° N, longitude 9.23° E, altitude 137 m a.m.s.l.) an experimental station with two receivers recording the beacon power at 8 samples/second with approximately 30 dB of dynamic range. The Alphasat satellite is tracked using a step motor, which is moved on the basis of the ephemeris information provided on a weekly basis by Inmarsat (which operates the satellite). The average link elevation angle in Milan is 35.6°, while the diameter of the receiving antennas is 1.2 m (Ka band) and 0.6 m (Q band). Collocated with the beacon receivers are also a laser-based disdrometer to measure the rain rate [16] with 1-minute integration time and a Ka-/W-band microwave radiometer (MWR) to support the derivation of the tropospheric attenuation from the received beacon power [17]. The beacon data availability in the period considered in this work is approximately 92% for both bands.

B. Madrid

The GTIC–Radiocommunication Research Group of the UPM currently manages two satellite experiments in Madrid: the Ka-band experiment (receiving the Ka-band signal emitted from the KA-SAT geostationary satellite located at 9° E) and the Q-band experiment (receiving the Q-band signal broadcast from the Alphasat satellite). The latter is part of the Alphasat Aldo Paraboni propagation experiment. Both beacon receivers were built at UPM and are located on the rooftop of a UPM building (latitude 40.45° N, longitude 3.73° W altitude 680 m a.m.s.l.). Ancillary equipment, i.e. an automatic meteorological station, a rain gauge, an optical disdrometer (the data from both rain sensors operate with 1-minute integration time) and a vertically-pointed Doppler radar, were installed near the receivers.

The Ka-band beacon receiver (originally designed for the HB-6 satellite) utilizes a 1.2-m Centered Cassegrain antenna pointed at 160.81° of azimuth and 41.41° of elevation, and receives the 19.68 GHz horizontally polarized signal with a tilt from the horizon of 19°. The signal amplitude is measured by a digital PLL-based (Phase-Locked Loop) receiver and sampled at 18.66 samples/s. The receiver dynamic range is of approximately 30 dB. The detailed data processing and more setup characteristics can be consulted in [18]. The data availability is 97% for the 5-year period (from September 2013 to October 2018) of concurrent rain and attenuation measurements.

The Q-band beacon receiver, whose dynamic range varied from 35 to 38 dB during the measurement period, is oriented towards the Alphasat satellite [15], receiving the 39.4-GHz linearly polarized beacon signal with a tilt of 90°. Since the satellite orbit is not geostationary, the 0.9-m centered parabolic antenna was mounted on a commercial motorized head that allows an accurate pointing (having mean values of 139.5° in azimuth and 34.5° in elevation). A MATLAB-based application was developed to control the antenna steering direction, using either Two-Line Element (TLE) or Orbit Ephemeris Message (OEM) files. The signal and noise levels are calculated in real time using a Fast Fourier Transform (FFT)-based algorithm with a sampling frequency of 18.78 samples/s. A more detailed description about the experimental configuration and data processing can be found in [19]. The 5-year period of concurrent rain and attenuation data covers the months from March 2014 to March 2019, excluding March 2017, with a data availability of 96%.

C. Spino d'Adda

The ITALSAT experiment was promoted and funded by the Italian Space Agency. ITALSAT was a three-axes stabilized satellite in a geostationary orbit at 13° E longitude, which carried a propagation payload featuring three beacons at 18.7 (vertical polarization), 39.6 (circular polarization), and 49.5 GHz (switched polarization between horizontal and vertical). Receiving stations were installed in a few sites across Europe, including Spino d'Adda (latitude 45.4° N, longitude 9.5° E, altitude 84 m a.m.s.l.), close to Milan, Italy [5], where a ground terminal featuring a 3.5-m diameter antenna and a dynamic range of 40 dB was used to collect eight years of propagation data (1993-2000, with data availability higher than 90% for the three bands) with 1-second sampling time, at the three frequencies, and with 37.7° elevation angle. The propagation data were processed by the Consiglio Nazionale delle Ricerche (CNR) and Politecnico di Milano. Concurrent measurements of the rain rate (1-minute integration time) were collected in the same site using a high-resolution tipping bucket rain gauge, while a 3-channel Ku-/Ka-band MWR aided the calculation of the tropospheric attenuation in non-rainy conditions.

Table I summarizes the main electrical and geometrical features of the links included in the experimental campaign conducted in Milan, Madrid and Spino d'Adda.

TABLE I. GEOMETRICAL AND ELECTRICAL FEATURES OF THE LINKS INCLUDED IN THE EXPERIMENTAL CAMPAIGN CONDUCTED IN MILAN, MADRID AND SPINO D'ADDA.

SITE	FREQUENCY	ELEVATION ANGLE	POLARIZATION
Milan	19.7 GHz	35.6°	Linear V
	39.4 GHz	35.6°	Linear tilted 45°
Madrid	19.68 GHz	41.4°	Linear tilted 19°
	39.4 GHz	34.5°	Linear tilted 90°
Spino d'Adda	18.7 GHz	37.7 °	Linear V
	39.6 GHz	37.7 °	RHCP
	49.5 GHz	37.7 °	V/H switched at 933 Hz

III. DATA PROCESSING

This Section describes how the propagation data were processed in the three sites to obtain the joint rain rate and rain attenuation statistics, to be used as input to TD-SCEX and as a reference to evaluate its accuracy, respectively.

A. Rain Rate Time Series

In this work, the rain rate information is key for different reasons. In first instance, the temporal evolution of the rain intensity helps identify rain events affecting the Earth-space link, which, in turn, allows obtaining the rain attenuation from the beacon-derived total tropospheric attenuation (see Section III.B below); secondly, the rain rate time series are used to calculate the joint complementary cumulative distribution functions (CCDFs), for a set of time lags, to be used as input to SC EXCELL. According to the main concept on which time diversity relies, this is achieved by adding to each rain rate time series a copy shifted ahead in time by a time lag Δt, and by selecting, each minute, the minimum rain rate between the original and the shifted time series. This is clarified in Fig. 1 for a rain event occurred in Milan on the 1st November 2018: in this case, Δt = 50 minutes.

The joint rain rate CCDFs are calculated for the three sites using different time lag values and the whole rain rate datasets. As an example, Fig. 2 depicts the results obtained at Milan (data collected in 2017 and 2018): as expected the rain rate decreases as the time lag increases.

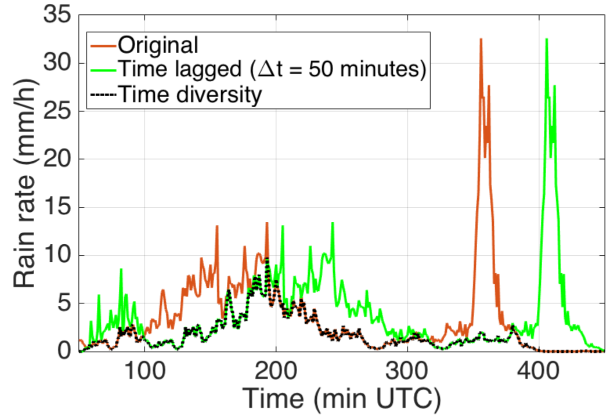

Fig. 1. Illustration of how the time diversity rain rate time series (black dashed line) is calculated from the original time series (red solid line) and its lagged copy (green solid line); the example refers to a rain event occurred in Milan on the 1st November 2018, using Δt = 50 minutes.

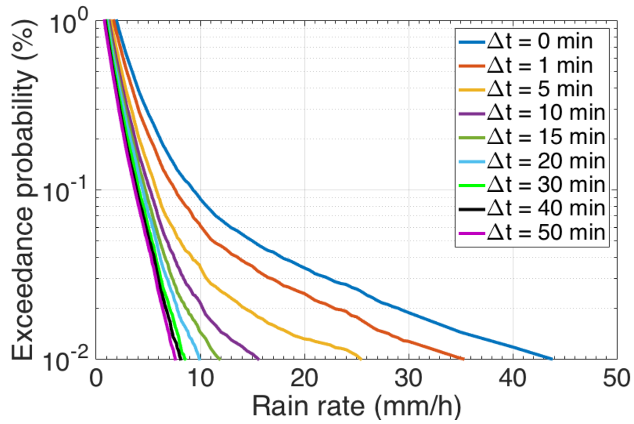

Fig. 2. Joint rain rate CCDFs obtained from the whole rain rate dataset available in Milan (2017-2018).

B. Beacon Data

Rain attenuation time series are obtained by processing the received beacon power using a common procedure in the three sites. The first step consists in low-pass filtering the received beacon power P_b to remove scintillations with typical cut-off frequency of 0.03 Hz [20]. Then, rain events are identified, both by taking advantage of the local rain rate and by visually inspecting the trend of P_b, i.e. by searching for the sudden decrease in the received power at both bands. The final step to isolate the attenuation due to rain is to subtract from P_b the power level that is the linear interpolation of P_b just before the beginning and just after the end of each event [21].

Afterwards the rain attenuation time series are processed to produce the joint CCDFs to be used as reference to test the accuracy of TD-SCEX. This is achieved using the same approach outlined for rain rate data. In addition, the attenuation data are carefully checked to identify outage periods and the joint rain attenuation CCDFs are obtained as follows (considering e.g. the time lag Δt = 30 minutes): 1) if the samples at time t_0 and $t_0+\Delta t$ are both associated to outage (very rare case), they are excluded; 2) if the samples at time t_0 is associated to outage and the one at $t_0+\Delta t$ is not, the former is included in the CCDF with Δt = 0 after replacing it with a value beyond the receiver dynamic range, and the latter is included in the joint CCDF with Δt = 30; 3) if the samples at time t_0 is not associated to outage and the one at $t_0+\Delta t$ is, the former is included in both CCDFs with Δt = 0 and with Δt = 30 minutes.

It is worth pointing out that, while deriving the joint CCDFs of rain attenuation and rain rate, the concurrent availability of both types of data was taken into account to guarantee a consistent comparison between the outputs of SC EXCELL and the beacon-derived statistics. As an example, Fig. 3 reports the joint rain attenuation CCDFs at Q band at Milan (2017-2018).

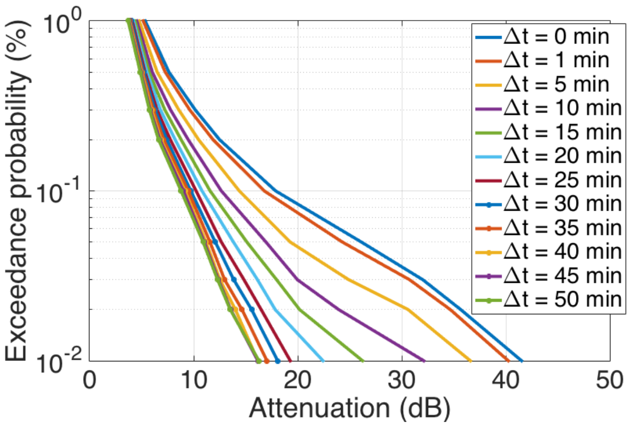

Fig. 3. Joint rain attenuation CCDFs obtained from the whole rain attenuation dataset available in Milan (2017-2018) at Q band.

IV. Time Diversity Prediction Model

A. The SC EXCELL model

The methodology proposed in this work to predict the advantage originating from the implementation of time diversity is underpinned by the SC EXCELL model. Firstly presented in [13] (and updated in [22]) as an enhancement of the original EXCELL model [23], SC EXCELL predicts the rain attenuation affecting Earth-space links by relying on a simple analytical expression to model the real rain cells observed in weather-derived precipitation maps. Each synthetic cell is identified by the peak rain intensity (R_M), whose value R decays exponentially with the distance from the cell center ρ, with a slope that is regulated by the equivalent cell diameter (ρ_0):

$$R(\rho) = R_M e^{-\frac{\rho}{\rho_0}} \quad (1)$$

The population of rain cells in a site, i.e. the probability that a given type of cell is present, $N(R_M,\rho_0)$, is tightly linked to the local rain rate CCDF, also typically referred to as $P(R)$:

$$N(R_M,\rho_0) = -\frac{1}{4\pi \overline{\rho_0}^2} \frac{\partial^3 P^*(R)}{\partial \ln(R+R_{low})^3} e^{-\frac{\rho_0}{\overline{\rho_0}}} \quad (2)$$

In (2), the average equivalent cell diameter is given by:

$$\overline{\rho_0}(R_M) = 1.7\left[\left(\frac{R_M}{6}\right)^{-10} + \left(\frac{R_M}{6}\right)^{-0.26}\right] \quad (3)$$

while $P^*(R)$ is the following analytical expression, whose parameters P_0, R_{asint}, R_{low} and n are regressed using a best-fit procedure aimed at maximizing the agreement between $P^*(R)$ and the input $P(R)$:

$$P^*(R) = P_0 \ln^n\left(\frac{R_{asint}+R_{low}}{R+R_{low}}\right) \quad (4)$$

The key advancement of SC EXCELL over EXCELL is the chance to consider the different impact of stratiform and convective precipitation on the link. In fact, using a threshold on R_M (which also depends on the site, as explained in [24]), rain cells are labelled as stratiform or convective, and thus associated to different rain heights:

$$h_{str} = \frac{\sum_{i=1}^{12}\alpha_i p_i h_i}{\sum_{i=1}^{12}\alpha_i p_i} \qquad h_{cnv} = \frac{\sum_{i=1}^{12}\beta_i p_i h_i}{\sum_{i=1}^{12}\beta_i p_i} \quad (5)$$

where h_i (km) is the monthly mean values of the 0 °C isotherm height, p_i is the monthly mean value of the 6-hour rainy periods probability, β_i is the monthly mean value of the ratio between the convective and the total rain amounts, $\alpha_i = 1-\beta_i$ and, finally, i = 1,..,12 is the month index. All the data in (5) are extracted from the ERA40 dataset, produced globally by the European Centre for Medium-Range Weather Forecast (ECMWF) [25]. As a result, the rain heights for stratiform and convective rain cells are:

$$H_{str}(f) = h_{str} + H_{BB}(f) \qquad H_{cnv} = 1.1 h_{cnv} \quad (6)$$

Note that the convective rain height H_{cnv} includes a factor increasing h_{cnv} to take into account, in an equivalent way, that during convective events, rain drops extend beyond the 0 °C isotherm height due to the strong updrafts and downdrafts characterizing that type of event; on the other hand, the dissipative contribution of the bright band is added only during stratiform events, in terms of an additional equivalent frequency dependent rain height $H_{BB}(f)$ [22]:

$$H_{BB}(f) = 4.454\, e^{-0.0656 f} + 0.826 \quad (7)$$

The attenuation induced by each rain cell is calculated by simulating the interaction of such a cell with the Earth-space link, as explained in detail in [23]; to this aim, besides all the data required for the implementation of equations (1)-(7), SC EXCELL also receives as input the wave polarization, the elevation angle, the operational frequency, all of which are used to extract from recommendation ITU-R P.838-3 the k and α power law coefficients used to turn the rain rate into specific rain attenuation [26]. Finally, the attenuation values coming from each synthetic cell are all cumulated to derive the CCDF of the rain attenuation.

B. The SC EXCELL model for the prediction of the time diversity gain

The satisfactory accuracy achieved by SC EXCELL in predicting the CCDF of the rain attenuation affecting Earth-space links (e.g. see the tests in [13] and [22]) prompted us to explore its applicability (and its performance) also to scenarios involving time diversity systems. To this aim, in practical terms, SC EXCELL is applied as is, i.e. using the procedure

The final version of record is available at http://dx.doi.org/10.1109/TAP.2021.3061176

and equations illustrated in Section IV.A, though with just one different input: instead of using the customary mean yearly $P(R)$, the model is fed with one of the joint time diversity rain rate statistics, e.g. reported in Fig. 2 for Milan. In fact, the information on the temporal decorrelation of rainfall is inherently embedded in such joint statistics, which, in turn, regulate the generation of the local rain cell population through (2): as the time lag increases, the input $P(R)$ will be characterized by rain rate values that tend to decrease (see Fig. 2), thus giving rise to less intense rain cells, i.e. reduced attenuation values. This is confirmed by the results reported in Fig. 4, which shows, as an example, the application of SC EXCELL for time diversity predictions in Milan at Ka band.

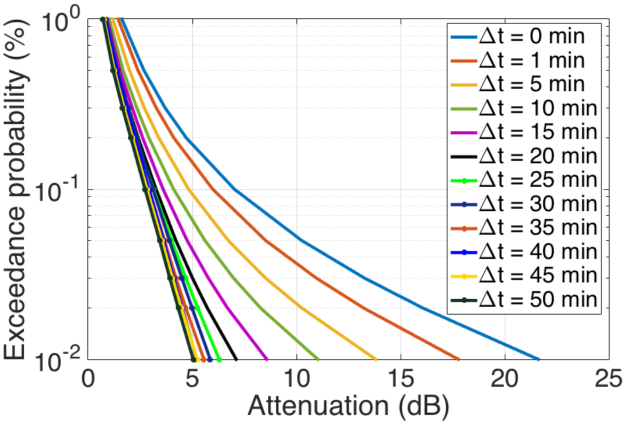

Fig. 4. Joint rain attenuation CCDFs predicted by TD-SCEX: Milan, Ka band.

V. Results and Discussion

This section presents the tests aimed at validating the application of SC EXCELL to scenarios involving time diversity systems. The model accuracy is evaluated both on the joint rain attenuation CCDFs and on the time diversity gain.

A. Joint Rain Attenuation CCDFs

TD-SCEX was applied to obtain results in the three sites where propagation measurements are available, using as input to SC EXCELL the joint rain rate CCDFs calculated in Section III.A and the link parameters listed in Table I. The maximum time lag considered for the tests is 50 minutes: in fact, as shown both in Fig. 3, increasing the time lag from 45 to 50 minutes brings almost no incremental advantage in using time diversity, and even less would with a longer time lag. As examples, Fig. 5, Fig. 6 and Fig. 7 show the outputs of the model, which are compared to the joint statistics derived from the beacon measurements. More specifically, Fig. 5 refers to the Ka-band data in Milan for Δt = 50 min, Fig. 6 reports the results for the Q-band data in Madrid with Δt = 10 min, while Fig. 7 depicts the comparison for the V-band data collected in Spino d'Adda with Δt = 30 min.

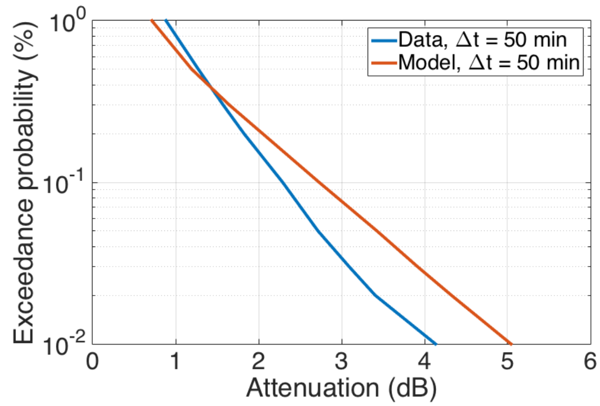

Fig. 5. Joint rain attenuation CCDFs predicted by TD-SCEX (red line) and calculated from the Ka-band data collected in Milan (blue line); retransmission delay equal to 50 minutes.

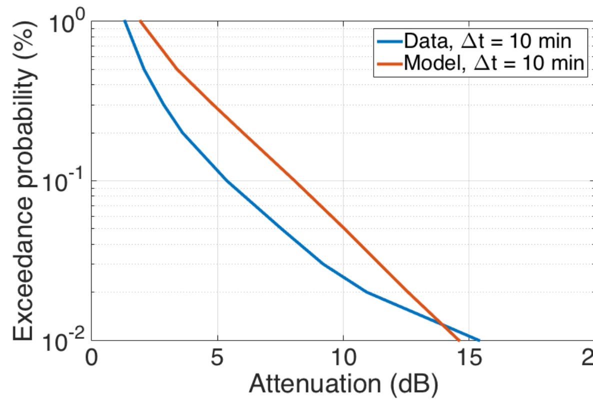

Fig. 6. Joint rain attenuation CCDFs predicted by TD-SCEX (red line) and calculated from the Q-band data collected in Madrid (blue line); retransmission delay equal to 10 minutes.

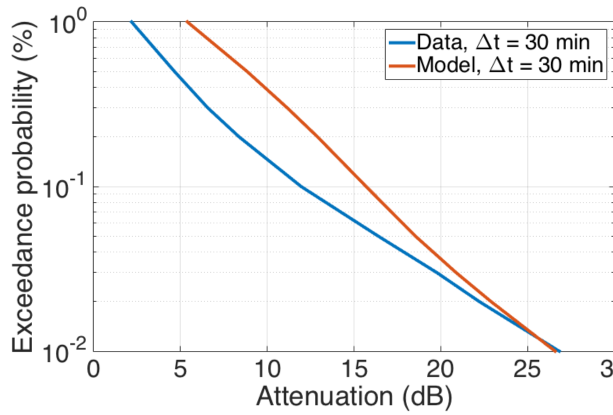

Fig. 7. Joint rain attenuation CCDFs predicted by TD-SCEX (red line) and calculated from the V-band data collected in Spino d'Adda (blue line); retransmission delay equal to 30 minutes.

The results reported in Fig. 5, Fig. 6 and Fig. 7 indicate quite a good prediction accuracy, which can be assessed quantitatively by using the figure of merit ε, typically used to compare rain attenuation statistics [27]:

$$\varepsilon(P) = \begin{cases} \left(\frac{A_R(P)}{10}\right)^{0.2} \ln\left(\frac{A_P(P)}{A_R(P)}\right) & A_R(P) < 10 \text{ dB} \\ \ln\left(\frac{A_P(P)}{A_R(P)}\right) & A_R(P) \geq 10 \text{ dB} \end{cases} \quad (8)$$

where $A_R(P)$ and $A_P(P)$ are the rain attenuation values extracted from the measured and predicted CCDFs, respectively, both for the same exceedance probability *P*. The values of ε over the full 0.01%-1% probability range are used to calculate the statistical parameters for each set of curves, specifically the *P* values recommended by ITU-R ([1% 0.5% 0.3% 0.2% 0.1% 0.05% 0.03% 0.02% 0.01%]) [27].

Fig. 8 to Fig. 10 depict the average (E) and root mean square (RMS) value of ε as a function of the time lag Δt; more in detail, each figure refers to a specific frequency band (Ka, Q and V, respectively) and it includes the results from all the sites (where available). The best prediction results are achieved in Milan, with a maximum RMS below 0.2 and 0.1, at Ka band and Q band, respectively. On the contrary, the worst results are obtained for Madrid at both bands (RMS around 0.3 on average). In Spino d'Adda, the error increases with the increasing frequency. As general observations, the error tends to increase for longer time lags and the model often overestimates the rain attenuation CCDFs, save for the data collected in Madrid at Ka band.

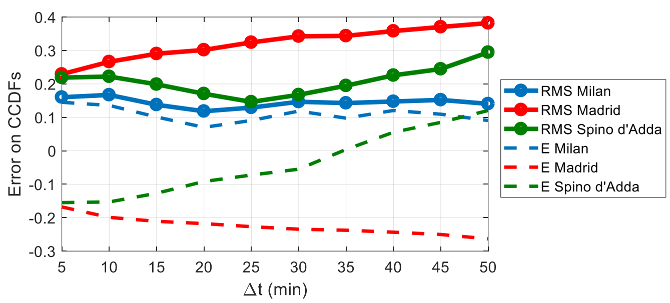

Fig. 8. E (dashed lines) and RMS (solid lines with markers) of the error on joint rain attenuation CCDFs as a function of time lag: Ka band in Milan (blue line), Madrid (red line) and Spino d'Adda (green line).

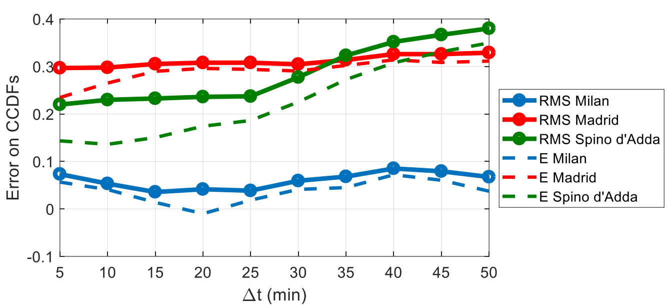

Fig. 9. E (dashed lines) and RMS (solid lines with markers) of the error on joint rain attenuation CCDFs as a function of time lag: Q band in Milan (blue line), Madrid (red line) and Spino d'Adda (green line).

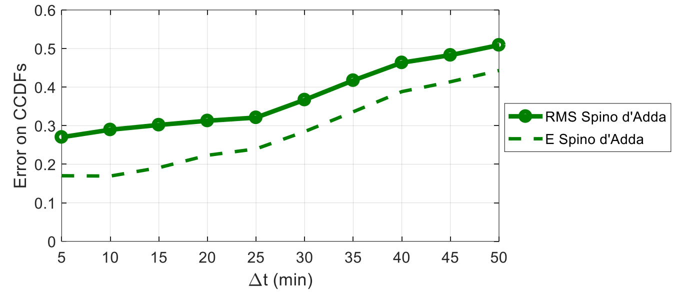

Fig. 10. E (dashed lines) and RMS (solid lines with markers) of the error on joint rain attenuation CCDFs as a function of time lag: V band in Spino d'Adda.

B. Diversity Gain Analysis

The performance of TD-SCEX is evaluated also in terms of the diversity gain *G*, defined as:

$$G(\Delta t, P) = A_s(P) - A_J(\Delta t, P) \quad (9)$$

where $A_S(P)$ is the rain attenuation value, for the exceedance probability level *P*, extracted from the rain attenuation CCDF associated to the system without time diversity, while A_J is the same value but associated to the joint rain attenuation CCDF at time lag Δt. The calculation of the time diversity gain is clarified in Fig. 11 for a sample time lag of 35 minutes.

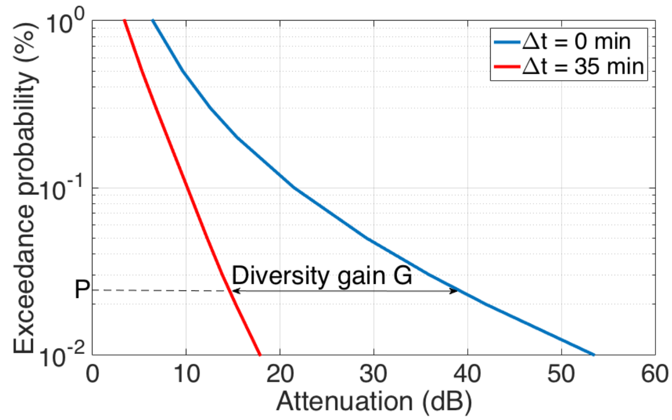

Fig. 11. Definition of the diversity gain *G* for the generic outage probability level *P*.

As an example, Fig. 12 compares the *G* values predicted by the model (dashed lines) and calculated from the Ka-band data collected in Milan. Each pair of curves with the same color refers to a given exceedance probability value *P* ranging between 0.01% and 0.1%. The *G* values derived from the model's predictions and from the measurements follow the same trend: as expected, the gain increases rapidly as *P* decreases; the same occurs, for a fixed value of *P*, with the increase in Δt. In particular, *G* increases steeply for time lags up to 25 minutes, which is related to the fast temporal decorrelation of rainfall, especially typical of short but intense rain events. For Δt > 25 minutes, *G* still increases, but at a slower pace, until it reaches quite a stable value around Δt = 40-50 minutes.

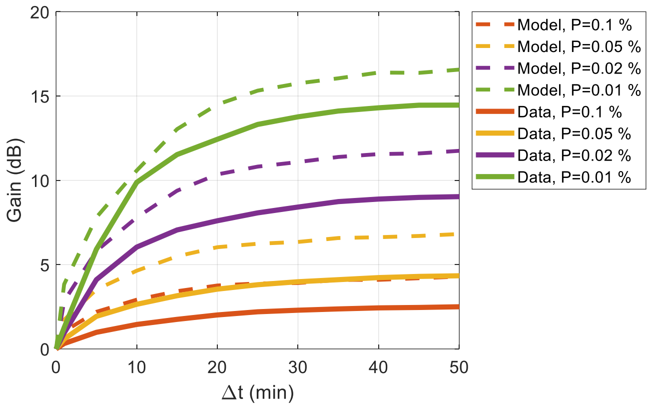

Fig. 12. Diversity gain G as a function of the time lag and of the exceedance probability P: comparison between model's predictions (dashed lines) and data-derived values (solid lines) at Ka band in Milan for P equal to 0.1% (red), 0.05% (yellow), 0.02% (violet) and 0.01% (green).

Fig. 13 reports similar results as Fig. 12, but for Madrid at Q band: in this case, the model's outputs are accurate up to approximately $\Delta t = 10$ minutes, after which the agreement between the predicted and measured curves decreases, though still maintaining the same trend.

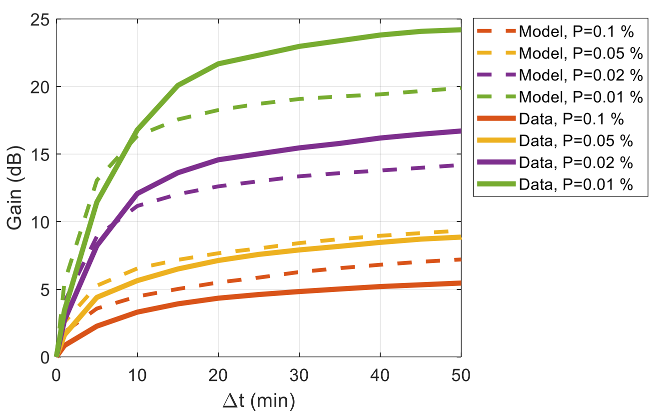

Fig. 13. Diversity gain G as a function of the time lag and of the exceedance probability P: comparison between model's predictions (dashed lines) and data-derived values (solid lines) at Q band in Madrid for P equal to 0.1% (red), 0.05% (yellow), 0.02% (violet) and 0.01% (green).

Finally, Fig. 14 depicts the comparison between predictions and measurements collected at V band in Spino d'Adda: the increase in G with the time lag is clearly more gradual than the one reported in Fig. 13 for Madrid. Such a difference in the gains measured in Madrid and in the Italian sites is likely ascribable to the different climatic features of the two regions. Madrid lies on a plateau at 650 m a.m.s.l. located at the center of the Iberian Peninsula: the climate is continental, with dry and hot summers, mild winters, and a low mean precipitation level (440 mm/year). On the other hand, Milan is more influenced by the Mediterranean sea (it lies roughly at 115 km from the coast), is sheltered by the Alps from the cold Northern winds and it experiences a higher mean yearly rain amount (between 700 and 800 mm). As a result of the climatic differences, though both sites are subject to both stratiform and convective rain events, the latter are likely more frequent, of higher intensity and of shorter duration in Madrid than those affecting Milan and Spino d'Adda.

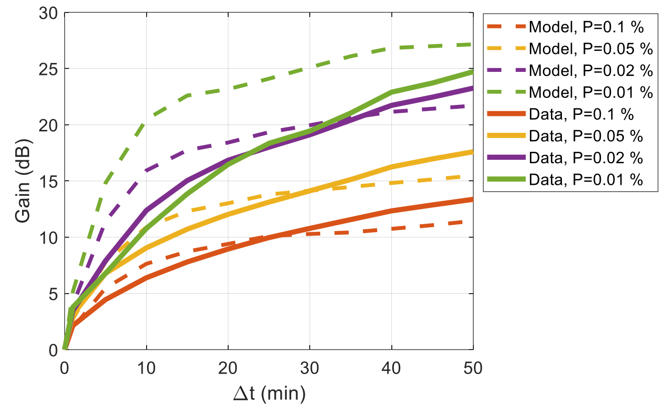

Fig. 14. Diversity gain G as a function of the time lag and of the exceedance probability P: comparison between model's predictions (dashed lines) and data-derived values (sold lines) at V band in Spino d'Adda for P equal to 0.1% (red), 0.05% (yellow), 0.02% (violet) and 0.01% (green).

As a complement to the previous prediction examples, Fig. 15, Fig. 16 and Fig. 17 summarize the overall results by showing the E and RMS of ε as a function of the time lag: in this case, ε is defined as in equation (8), but the attenuation values are replaced with the gain values.

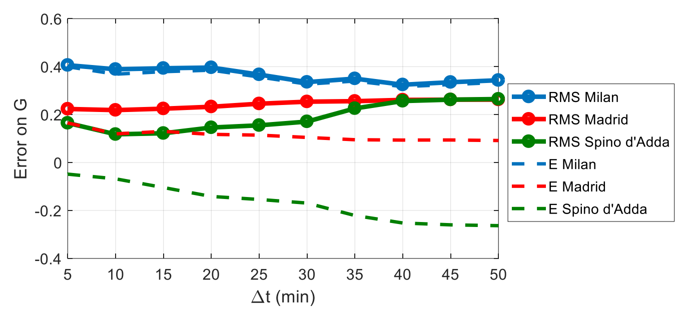

Fig. 15. E (dashed lines) and RMS (solid lines with markers) of the error on the time diversity gain as a function of time lag: Ka band in Milan (blue line), Madrid (red line) and Spino d'Adda (green line).

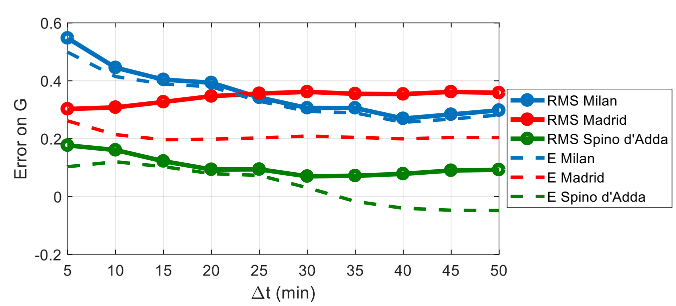

Fig. 16. E (dashed lines) and RMS (solid lines with markers) of the error on the time diversity gain as a function of time lag: Q band in Milan (blue line), Madrid (red line) and Spino d'Adda (green line).

The final version of record is available at http://dx.doi.org/10.1109/TAP.2021.3061176

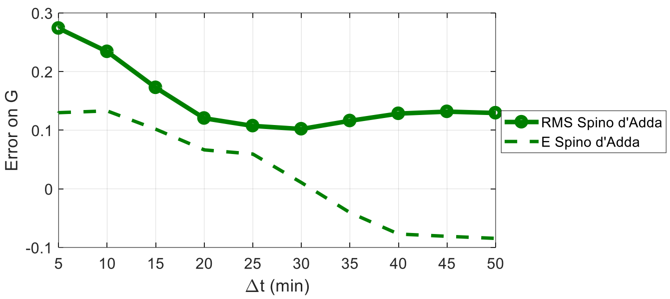

Fig. 17. E (dashed lines) and RMS (solid lines with markers) of the error on the time diversity gain as a function of time lag: V band in Spino d'Adda.

The model tends to overestimate the diversity gain, save for the data collected in Spino d'Adda: in this case, the E is either always negative (Ka band) or it goes from positive to negative as the time lag increases. More in general, the performance results on the time diversity gain turn out to be opposite to those obtained on the CCDFs error: the lowest RMS values are achieved in Spino d'Adda and they are quite stable with the frequency. The difference in the results on the CCDFs and on G can be explained by considering the different procedures for the calculation of the two errors: in the former case, as shown e.g. in Fig. 5, the error is directly calculated between the reference data and the curve predicted by the model, both associated to the same time lag; in the latter case, a further step is necessary before the comparison between predictions and data, i.e. the calculation of G as in Fig. 11 using either a set of reference curves or a pair of statistics predicted by the model.

C. Comparison with Other Models in the Literature

As a term of comparison for the accuracy results derived in Section V.A, the propagation data described in Section II were used also to test other models proposed in the literature to predict the advantage originating from the implementation of time diversity. Specifically, we have tested the following models:

- The Joint Probability Model (JPM) presented in [9], underpinned by an analytical expression to model the time correlation of rain attenuation as a function of the time lag, parameterized by regression on rain attenuation measurements.
- The prediction methods developed by Greece in [10], which also employs an analytical expression to model the time correlation of rain attenuation as a function of the time lag. Its main feature is the use of a statistical parameter β that describes the dynamical properties of rain attenuation along the propagation path.
- The model proposed by Matricciani in [6] (MM), which relies on a simple formula, in turn dependent on the frequency and on the rain attenuation CCDF (Δt = 0 min).
- The ONERA model [11] (OM), which relies on the conversion of a stationary-correlated Gaussian process into a lognormal (rain attenuation) process.

Fig. 18 and Fig. 19 report the comparison among the models by showing the RMS of the error on the CCDFs as a function of the time lag, obtained using the Ka-band data and the Q-band data collected in Madrid, respectively. In the former case, TD-SCEX offers an accuracy slightly lower than the one delivered by the JPM; the best results are achieved by the MM, while much higher errors are associated to the GM and the OM. At Q band, the best and worst models are the JPM and the OM, respectively, while TD-SCEX offers results comparable to those of the GM and MM for longer time lags ($\Delta t \geq 35$ min).

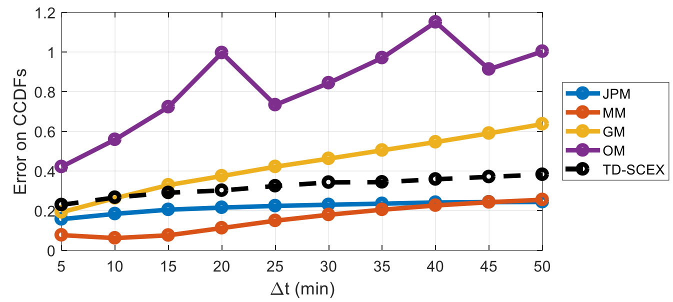

Fig. 18. RMS of the error on the joint rain attenuation CCDFs : comparison among the different models using the Ka-band data collected in Madrid.

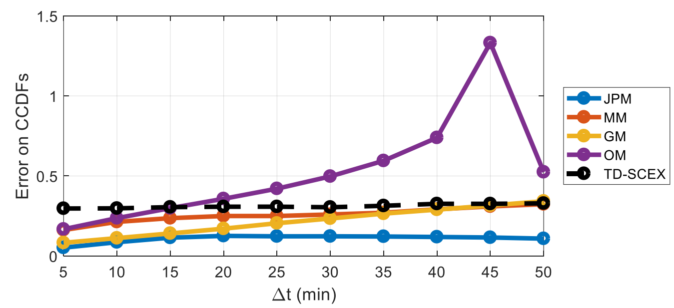

Fig. 19. RMS of the error on the joint rain attenuation CCDFs: comparison among the different models using the Q-band data collected in Madrid.

Fig. 20 and Fig. 21 extend the model comparison to the data collected in Milan by showing the results on Ka-band and Q-band data, respectively: TD-SCEX offers the best prediction accuracy for $\Delta t \geq 15$ min at Ka band, and $\Delta t \geq 10$ min at Q band. For lower time lags, the performance of TD-SCEX is still comparable to that achieved by the other models. In addition, at both bands, the OM provides the highest error for most of the time lags (all at Ka band, $\Delta t \geq 25$ min at Q band).

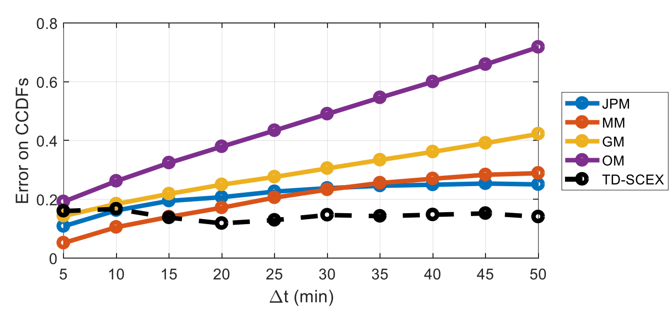

Fig. 20. RMS of the error on the joint rain attenuation CCDFs: comparison among the different models using the Ka-band data collected in Milan.

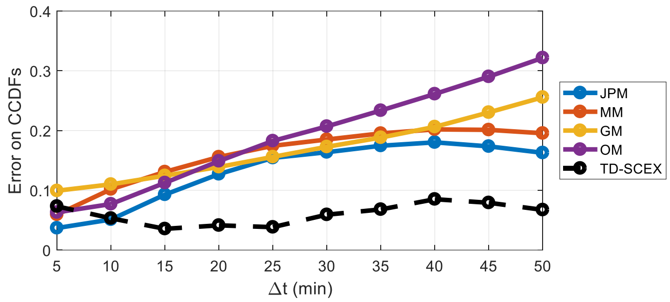

Fig. 21. RMS of the error on the joint rain attenuation CCDFs : comparison among the different models using the Q-band data collected in Milan.

The model comparison is completed by Fig. 22, Fig. 23 and Fig. 24, which depict the results obtained by using the ITALSAT data collected in Spino d'Adda, at Ka-band, Q-band and V-band, respectively. At Ka band, TD-SCEX offers a higher error for shorter time lags ($\Delta t \leq 15$ min), which, however, decreases significantly for $\Delta t \geq 20$ min, reaching the same low values also associated to the OM. On the other hand, both at Q band and V band, TD-SCEX provides the lowest prediction accuracy, with the best models being overall the MM and OM.

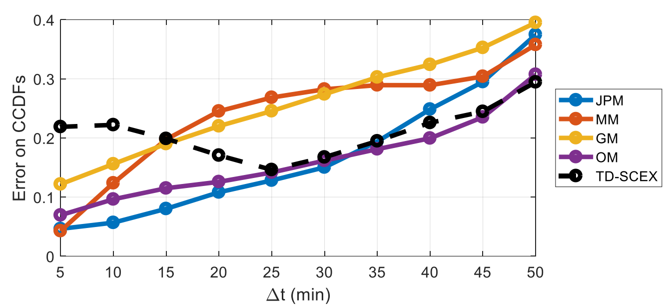

Fig. 22. RMS of the error on the joint rain attenuation CCDFs: comparison among the different models using the Ka-band data collected in Spino d'Adda.

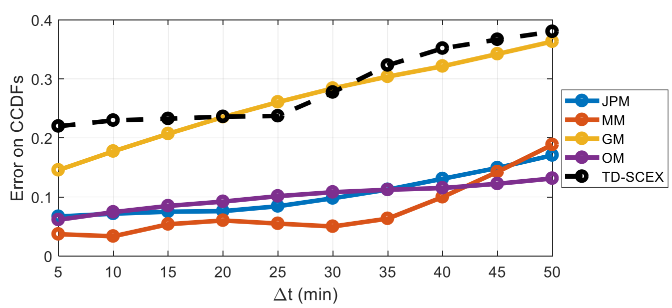

Fig. 23. RMS of the error on the joint rain attenuation CCDFs: comparison among the different models using the Q-band data collected in Spino d'Adda.

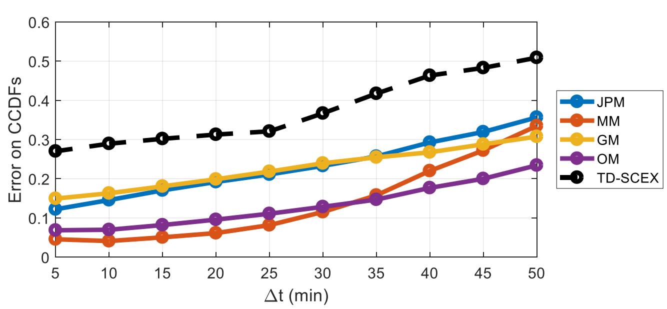

Fig. 24. RMS of the error on the joint rain attenuation CCDFs: comparison among the different models using the V-band data collected in Spino d'Adda.

In order to draw sensible conclusions on the models' accuracy, a key point on the comparison between TD-SCEX and the other prediction methods should be first highlighted. Indeed, all the models listed at the beginning of this Section require as input (at least) some information of the local rain attenuation CCDF. This is the case of the MM [6], while the other models rely on even more demanding inputs: the JPM additionally requires the joint rain attenuation CCDFs for several time lags in order to regress the necessary model's coefficients [9], while the GM and the OM cannot be duly parameterized without resorting to the local rain attenuation time series [10],[11]. On the contrary, the rain rate time series are the sole key input to TD-SCEX, which takes advantage of the SC EXCELL model to predict the effect of precipitation on the link (whose electrical and geometrical features must be known, obviously): in addition to the advantage of quite limited input requirements, TD-SCEX actually offers results comparable to those achieved by the other models.

VI. Conclusions

This work presents TD-SCEX, a new time diversity model that takes advantage of the SC EXCELL model to predict join time diversity rain attenuation statistics by receiving as input the joint time diversity rain rate statistics, as well as the geometrical and electrical characteristics of the link. TD-SCEX was tested against the propagation data collected in three sites (Milan, Madrid and Spino d'Adda) using beacon signals broadcast by three satellites (Alphasat, KA-SAT and ITALSAT) at three different bands (Ka, Q and V). The tests considered time lags Δt up to 50 minutes (using longer time lags does not bring a significant advantage to the system), and rain attenuation exceedance probability values between 0.01% and 1% (due to the limited statistical stability of the Milan experimental data for lower probability values), but its applicability to wider ranges of Δt and P is not prevented by any limitation in the model.

The tests on the accuracy of the model in estimating joint rain attenuation CCDFs indicate that the best predictions are achieved in Milan, with a maximum RMS below 0.2 and 0.1, at Ka band and Q band, respectively. On the contrary, the worst results are obtained for Madrid at both bands but overall not too far from the values obtained in the other sites (RMS around 0.3 on average). In Spino d'Adda, the error increases with the increasing frequency, as well as for longer time lags. Regarding the time diversity gain G, the model correctly predicts its increase with the time lag. More in general, the performance results on G turn out to be opposite to those obtained on the CCDFs error: the lowest RMS values are achieved in Spino d'Adda and they are quite stable with the frequency. When compared against other prediction models available in the literature, in addition to the advantage of more limited input requirements (the only key one being rain rate time series), TD-SCEX offers results in line with those achieved by the other models.

Overall, results indicate that TD-SCEX is a useful tool to predict the effectiveness of time diversity in mitigating the extreme fades induced by the atmosphere on EHF Earth-space communication systems: indeed, the overall good prediction results achieved by TD-SCEX when tested using data collected in two different regions are a hint of the robustness of the model against diverse climatic environments.

ACKNOWLEDGMENT

The authors would like to acknowledge: the Agenzia Spaziale Italiana (ASI), in particular Giuseppe Codispoti, for supporting the Alphasat Aldo Paraboni propagation experiment; NASA for making available the experimental data within the collaboration with Politecnico di Milano on the Alphasat Aldo Paraboni propagation experiment.

REFERENCES

[1] R. K. Crane, "Electromagnetic Wave Propagation Through Rain," New York, Wiley, 1996.

[2] A. D. Panagopoulos, P.-D. M. Arapoglou, and P. G. Cottis, "Satellite communications at Ku, Ka, and V bands: Propagation impairments and mitigation techniques," IEEE Commun. Surveys Tutorials, vol. 6, no. 3, pp. 2–14, 2004.

[3] Fukuchi H, Nakayama T. , "Quantitative evaluation of time diversity as a novel attenuation mitigation technology for future high speed satellite communication". IEICE Trans Commun 2004; E87-B(8):2119–2123.

[4] D. Pimienta-del-Valle, J. M. Riera, P. Garcia-del-Pino, "Time and Orbital Diversity assessment with Ka- and Q-Band slant-path propagation experiments in Madrid," IEEE Transactions on Antennas and Propagation, vol. 67, no. 2, pp. 1193-1201, 2019.

[5] C. Riva, "Seasonal and diurnal variations of total attenuation measured with the ITALSAT satellite at Spino d'Adda at 18.7, 39.6 and 49.5 GHz", International Journal of Satellite Communications and Networking, No. 22, 2004, pp. 449–476.

[6] E. Matricciani, "Time diversity as a rain attenuation countermeasure in satellite links in the 10-100 GHz frequency bands", EuCAP 2006, 6-10 November, 2006, Nice, France.

[7] L. Luini, C. Capsoni, "MultiEXCELL: a new rain field model for propagation applications," IEEE Transactions on Antennas and Propagation, vol. 59, no. 11, Page(s): 4286 - 4300, November 2011.

[8] L. Luini, C. Capsoni, "Preliminary Results From a Physically-Based Methodology for the Evaluation of a Time Diversity System", EuCAP 2011, pp. 1-5, 11-15 April 2011, Rome, Italy.

[9] V. Fabbro, L. Castanet, S. Croce, and C. Riva, "Characterization and modelling of time diversity statistics for satellite communications from 12 to 50 GHz", Int. J. Commun. Syst. Network, 27:87-101, 2009.

[10] Greece, "Information document on the prediction of time diversity in terrestrial LOS links operating above 10 GHz," ITU-R Study Group 3, input document 3K/68-3M/72, May 2009.

[11] ESA, "Development of high order propagation models for multimedia satellite communications systems," Final Report of ESA/ ESTEC Contract N° 40000107135/12/NL/LVH 2016.

[12] A. Rocha and S. Mota, "An Empirical Model for Time Diversity Statistics at Ka- and Q-band," in *EuCAP 2020*, Copenhagen, Denmark, 2020, pp. 1-5.

[13] C. Capsoni, L. Luini, A. Paraboni, A. Martellucci, "A New Prediction Model of Rain Attenuation That Separately Accounts for Stratiform and Convective Rain," IEEE Transactions on Antennas and Propagation, Vol 57, No. 1, Page(s): 196 – 204, January 2009.

[14] C. Capsoni, F. Fedi and A. Paraboni, "A comprehensive meteorologically oriented methodology for the prediction of wave propagation parameters in telecommunication applications beyond 10 GHz", Radio Science, vol. 22 (3), pp. 387-393, May-June 1987.

[15] T. Rossi, M. De Sanctis, M. Ruggieri, C. Riva, L. Luini, G. Codispoti, E. Russo, G. Parca, "Satellite Communication and Propagation Experiments Through the Alphasat Q/V Band Aldo Paraboni Technology Demonstration Payload," IEEE Aerospace and Electronic Systems Magazine, Vol. 31, No. 3, Page(s): 18 – 27, March 2016.

[16] Thies Clima Laser Precipitation Monitor: Instructions for Use. Rev. 2.5. July 2011.

[17] L. Luini, C. Riva, R. Nebuloni, M. Mauri, J. Nessel, A. Fanti, "Calibration and Use of Microwave Radiometers in Multiple-site EM Wave Propagation Experiments," EuCAP 2018, 9-13 April 2018, pp. 1-5, London, UK.

[18] J. M. Garcia-Rubia, J. M. Riera, P. Garcia-del-Pino, A. Benarroch, "Propagation in the Ka Band: Experimental Characterization for Satellite Applications," IEEE Antennas and Propagation Magazine, vol. 53, no. 2, pp. 65-76, April 2011.

[19] D. Pimienta-del-Valle, J. M. Riera, P. Garcia-del-Pino, G. A. Siles, "Three-year fade and inter-fade duration statistics from the Q-band Alphasat propagation experiment in Madrid," International Journal of Satellite Communication and Networking, vol. 37, no. 5, pp. 460-476, 2019.

[20] E. Matricciani, M. Mauri, C. Riva, "Scintillation and simultaneous rain attenuation at 12.5 GHz to satellite Olympus", Radio Science, vol. 32, no. 5, Pages: pp. 1861-186, September-October 1997.

[21] X. Boulanger, B. Benammar, L. Castanet, "Propagation Experiment at Ka-Band in French Guiana: First Year of Measurements," IEEE Antennas and Wireless Propagation Letters, Vol. 18, No. 2, pp. 241-244, 2019.

[22] C. Capsoni, L. Luini, "The SC EXCELL Model for the Prediction of Monthly Rain Attenuation Statistics", pp. 1382-1385, EuCAP 2013, 8-12 April 2013, Gothenburg, Sweden.

[23] C. Capsoni, F. Fedi, C. Magistroni, A. Paraboni, A. Pawlina, "Data and theory for a new model of the horizontal structure of rain cells for propagation applications," Radio Science, Volume 22, Number 3, Pages: 395-404, May-June 1987.

[24] C. Capsoni, L. Luini, A. Paraboni, C. Riva, "Stratiform and convective rain discrimination deduced from local $P(R)$," IEEE Transactions on Antennas and Propagation, vol. 54, issue 11, pp. 3566-3569, Nov. 2006.

[25] www.ecmwf.int. Accessed September 2020.

[26] Recommendation ITU-R P.838-3, "Specific attenuation model for rain for use in prediction methods," Geneva, 2005.

[27] ITU-R Study Group 3, "On testing variables used for the selection of prediction methods," ITU-R, Fascicle Document 3M/FAS/1-E, July 2016.